**JOURNAL OF THEORETICAL AND APPLIED MECHANICS**
**45**, 4, pp. 853-871, Warsaw 2007

# SIMULATION OF TRANSIENT FLOWS IN A HYDRAULIC SYSTEM WITH A LONG LIQUID LINE

Zbigniew Zarzycki
Sylwester Kudźma

*Szczecin University of Technology, Department of Mechanics and Machine Elements, Poland*
*e-mail: zbigniew.zarzycki@ps.pl; sylwester.kudzma@ps.pl*

Zygmunt Kudźma
Michał Stosiak

*Wrocław University of Technology, Institute of Machine Design and Operation, Poland*
*e-mail: zygmunt.kudzma@pwr.wroc.pl, michal.stosiak@pwr.wroc.pl*

The paper presents the problem of modelling and simulation of transients phenomena in hydraulic systems with long liquid lines. The unsteady resistance model is used to describe the unsteady liquid pipe flow. The wall shear stress at the pipe wall is expressed by means of the convolution of acceleration and a weighting function which depends on the (laminar or turbulent) character of the flow. The results of numerical simulation are presented for the waterhammer effect, which is caused by a sudden shift of the hydraulic directional control valve. The following cases of the system supply are considered: the first, with a constant delivery rate of the pump and the second, which additionally considers pulsation of the delivery of the pump. Computer simulations are compared with results of experiments. They are found to be very consistent in the case with the variable rate of the pump delivery taken into accent.

*Key words*: unsteady pipe flow, transients, waterhammer, pulsation of pump

## 1. Introduction

Drive and hydraulic control systems are often subjected to transient states, caused by dynamical excitation forces resulting either from sudden changes of the load of a motor or hydraulic actuator or else from changes of the flow

direction of the working liquid or speed caused by the control unit. It is often essential to precisely learn characteristics of dynamical runs in such states. It is very important in the design of automatic control systems or in the for analyzis of the strength of pipes and other elements of hydraulic systems.

While analyzing transient states, particular attention should be paid to such cases when a hydraulic system has a long liquid line (Garbacik and Szewczyk, 1995; Wylie and Streeter, 1978; Jelali and Kroll 2003), i.e. either when the length of the pipe is close to that of the pressure wave which is propagated in the system or when it is higher than that. Such a pipe is treated then as an element of a system with distributed parameters. Consequently, any changes of the flow pressure and rate are distributed along the pipes axis with a limited speed in the form of progressive and reflected waves.

In literature, the research of transient states concern mostly simple water-hammer cases (Wylie and Streeter, 1978; Ohmi *et al.*, 1985), in which simple boundary conditions are used. It means that at one end of the hydraulic line the pressure is constant (reservoir) and at the other, the velocity of flow equals zero (suddenly closed valve).

The present paper is an attempt at simulating transients caused by a sudden change of settings of the hydraulic control valve, with taking into account at the same time the pulsation delivery rate resulting from kinematics of a positive-displacement pump. The results obtained from numerical simulations are compared and validated with the recorded runs of pressure changes on a specially built test stand.

## 2. Mathematical model of the flow

The aim of the present paper is to present simulations of pressure transients of the considered system in cases of sudden jumps of pressure at the end of a long hydraulic line caused by e.g. operational overload.

The fundamental component of the hydraulic system, shown in Fig. 1, is the liquid long line which is treated as a distributed parameter element. The system is a subassembly, which is often found in many hydraulic systems of technical machinery and devices used e.g. in mining or ship building industry.

### 2.1. Fundamental equations

The unsteady flow in liquid pipes is often represented by two 1D hyperbolic partial differential equations. Linearized equations of momentum and

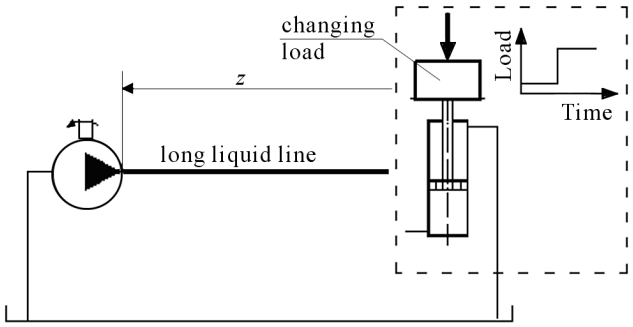


Fig. 1. The object of investigations

continuity can be given by Jungowski (1976), Ohmi *et al.* (1985) and Zarzycki (1994)

$$\rho_0 \frac{\partial v}{\partial t} + \frac{\partial p}{\partial z} + \frac{2}{R}\tau_w = 0 \qquad \frac{\partial p}{\partial t} + \rho_0 c_0^2 \frac{\partial v}{\partial z} = 0 \tag{2.1}$$

where: $t$ is time, $z$ – distance along the pipe axis, $v = v(z,t)$ – average value of velocity in a cross-section of the pipe, $p = p(z,t)$ – average value of pressure in a cross-section of pipe, $\tau_w$ – shear stress in the pipe wall, $\rho_0$ – density of the liquid (constant), $R$ – inner radius of the pipe.

The speed of the acoustic wave $c_0$ in Eq. $(2.1)_2$ takes into consideration compressibility of the liquid and elastic deformability of the pipe wall, and can be given by the following relation (Wylie and Streeter, 1978)

$$c_0 = \sqrt{\frac{\beta_c}{\rho_c}} \frac{1}{\sqrt{1 + 2\frac{\beta_c}{E}\frac{R}{g}}} \tag{2.2}$$

where $\beta_c$ is the bulk modulus of the liquid, $E$ – Young's modulus of the tube and $g$ – thickness of the wall.

In an unsteady flow in the pipe, the instantaneous stress $\tau_w$ may be regarded as a sum of two components: the quasi-steady state shear component and the unsteady state shear component (Ohmi *et al.*, 1985; Zarzycki, 2000)

$$\tau_w = \frac{1}{8}\lambda\rho_0 v|v| + \frac{2\mu}{R}\int_0^t w(t-u)\frac{\partial v}{\partial t}(u)\,du \tag{2.3}$$

where: $\lambda$ is the Darcy-Weisbach friction coefficient, $w$ – weighting function, $\mu$ – dynamic viscosity, $u$ – time used in the convolution integral.

The first component in Eq. (2.3) presents the quasi-steady state of the wall shear stress, the second one is the additional contribution due to unsteadiness.

The second summand in Eq. (2.3) relates the wall shear stress to the instantaneous average velocity and to the weighted past velocity changes. The system of Eqs. (2.1) and (2.3) is closed because of $p$ and $v$, as long as the weighting function $w(t)$ is known for the wall shear stress at the pipe wall.

### 2.2. Weighting functions

Zielke (1968) was first to give an analytical relation for the weighting function $w(t)$ for a laminar flow. He derived it from the analysis of a transient two-dimensional laminar flow. The Zielke model can be given by

$$w(\widehat{t}) = \begin{cases} \displaystyle\sum_{i=1}^{6} m_i \widehat{t}^{\frac{i-2}{2}} & \text{for} \quad \widehat{t} \leqslant 0.02 \\ \displaystyle\sum_{i=1}^{5} \exp(-n_i \widehat{t}) & \text{for} \quad \widehat{t} > 0.02 \end{cases} \tag{2.4}$$

where $m_i$ is 0.28209, $-1.25$, 1.05778, 0.93750, 0.396696, $-0.351563$ and $n_i = -26.3744$, $-70.8493$, $-135.0198$, $-218.9216$, $-322.5544$, respectively, and $\widehat{t}$ is the dimensionless time, defined by the following relation

$$\widehat{t} = \nu \frac{t}{R^2} \tag{2.5}$$

Zielke's model requires much computer memory and, therefore, it was modified by Trikha (1975) and Schoohl (1993) to improve its computational efficiency.

Schoohl's model can be given by

$$w(\widehat{t}) = \sum_{i=1}^{5} m_i \exp(-n_i \widehat{t}) \tag{2.6}$$

where: $m_1 = 1.051$, $m_2 = 2.358$, $m_3 = 9.021$, $m_4 = 29.47$, $m_5 = 79.55$, $n_1 = 26.65$, $n_2 = 100$, $n_3 = 669.6$, $n_4 = 6497$, $n_5 = 57990$.

In the case of the unsteady turbulent flow, the weighting function depends not only on the dimensional time but also on the Reynolds number. Vardy *et al.* (1993) and Vardy and Brown (1996) derived a model in which all viscosity effects were assumed to occur in the steady boundary layer (viscosity varied linearly across the outer annular shear layer). An approximated form of their weighting function model is

$$w_a = \frac{1}{2\sqrt{\pi \widehat{t}}} \exp\Big(-\frac{\widehat{t}}{C^*}\Big) \tag{2.7}$$

where

$$C* = \frac{12.86}{\mathrm{Re}^k} \qquad k = \log_{10} \frac{15.29}{\mathrm{Re}^{0.0567}}$$

Zarzycki (1994, 2000) developed a weighting function model using a four-region discretization (four instead of two regions) for turbulent viscosity distribution. The model had a complex mathematical form and it was further approximated to a simpler form

$$w_{apr} = C \frac{1}{\sqrt{\hat{t}}} \mathrm{Re}^n \tag{2.8}$$

where: $C = 0.299635,\ n = -0.005535$.

Zarzycki's model yields the same results as Vardy's model, but generates them more quickly. In Eq. (2.8), both time and Reynold's number (i.e. also the speed) are in the denominator, which makes calculations difficult. In order to eliminate these difficulties, Zarzycki and Kudźma (2004) and Kudźma (2005) presented a model similar to Schohl's model for a laminar flow. Their model can be given by

$$w_N(\hat{t}) = (c_1 \mathrm{Re}^{c_2} + c_3) \sum_{i=1}^{6} A_i \exp(-b_i \hat{t}) \tag{2.9}$$

where: $A_1 = 152.3936,\ A_2 = 414.8145,\ A_3 = 328.2,\ A_4 = 640.2165,\ A_5 = 58.51351,\ A_6 = 17.10735,\ b_1 = 207569.7,\ b_2 = 6316096,\ b_3 = 1464649,\ b_4 = 15512625,\ b_5 = 17790.69,\ b_6 = 477.887,\ c_1 = -1,5125,\ c_2 = 0.003264,\ c_3 = 2.55888$.

The value of critical Reynold's number (between unsteady laminar and turbulent flow), which qualifies the application of an appropriate weighting function, can be calculated by means of the following empirical relation (Ohmi *et al.*, 1985)

$$\mathrm{Re}_{cn} = 800\sqrt{\Omega} \tag{2.10}$$

Equation (2.10) can be used for an oscillatory flow, whereas for a pulsating flow $\mathrm{Re}_{cn}$ is (Ramaprian and Tu, 1980)

$$\mathrm{Re}_{cn} = 2100 \tag{2.11}$$

where: $\Omega = \omega R^2/\nu$ denotes the dimensionless frequency, $\omega = 2\pi/T$ – dimensional frequency, $T = 4L/c_0$ – period of the waterhammer, $L$ – length of the pipe.

For further simulations of the hydraulic waterhammer effect, two models were adopted: model (2.6) for the laminar flow and model (2.9) for the turbulent flow.

### 2.3. Method of characteristics. Computational codes

The system of Eqs. (2.1) and (2.3) with the known weighting function presents a closed nonlinear system of differential-integral Voltera's equations with a degenerated kernel. The system can be transformed into a pair of ordinary differential equations using MOC – a method of characteristics. As a result, we obtain (Zarzycki and Kudźma, 2004; Zarzycki and Kudźma, 2005)

$$\pm dp + \rho_0 c_0\, dv + \frac{2\tau_w c_0}{R}\, dt = 0 \qquad\qquad dz = \pm c_0\, dt \tag{2.12}$$

The net for the method of characteristics is shown in Fig. 2.

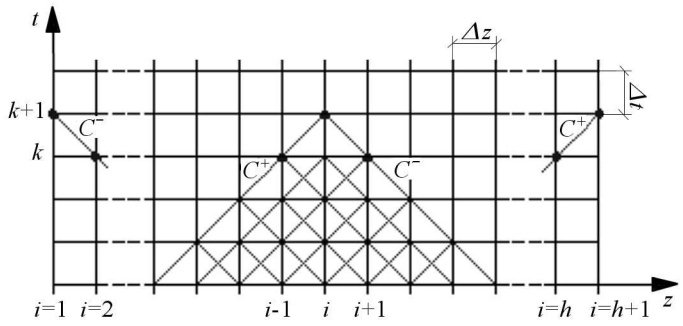


Fig. 2. The net of characteristics

Equations (2.12) were approximated using a differential scheme of the first order. As it was proved (Chaudhry and Hussaini, 1985) such an approximation gives satisfactory results provided that the time step $\Delta t$ remains small. Owing to that, a system of algebraic equations was created. The system enables calculation of cross-sectional mean values of the instantaneous pressure and flow rate:

— for the internal nodal points of the net of characteristics

$$\begin{aligned} p_{k+1,i} &= \frac{1}{2}\Big[(p_{k,i-1} + p_{k,i+1}) + \rho_0 c_0 (v_{k,i-1} - v_{k,i+1}) + \\ &\quad + \frac{2\Delta z}{R}(\tau_{w(k,i+1)} - \tau_{w(k,i-1)})\Big] \\ v_{k+1,i} &= \frac{1}{2}\Big\{(v_{k,i-1} + v_{k,i+1}) + \frac{1}{\rho_0 c_0}\Big[(p_{k,i-1} - p_{k,i+1}) + \\ &\quad + \frac{2\Delta z}{R}(\tau_{w(k,i+1)} + \tau_{w(k,i-1)})\Big]\Big\} \end{aligned} \tag{2.13}$$

— for the boundary nodal points of the net of characteristics:

$$\begin{aligned} p_{k+1,1} &= p_{k,2} + \rho_0 c_0 \Big[ (v_{k+1,1} - v_{k,2}) + \frac{2\Delta t}{R} \tau_{w(k,2)} \Big] \\ v_{k+1,h+1} &= v_{k,h} + \frac{1}{\rho_0 c_0} (p_{k,h} - p_{k+1,h+1}) - \frac{2\Delta t}{R} \tau_{w(k,h)} \end{aligned} \tag{2.14}$$

where $i = 2, 3, \ldots, h$, $k = 1, 2, \ldots, m$, $m$ is the number of time steps, $h$ – number of calculation sections along the hydraulic line.

As it was mentioned in Section 2.1, the instantaneous shear stress $\tau_w$ can be given by a sum of two components

$$\tau_{w(k,i)} = \tau_{wq(k,i)} + \tau_{wn(k,i)} \tag{2.15}$$

where

$$\begin{aligned} \tau_{wq(k,i)} &= \frac{1}{8} \rho_0 \lambda(\mathrm{Re}_{k,i}) v_{k,i} |v_{k,i}| \\ \tau_{wn(k,i)} &= \frac{2\mu}{R} [(v_{k,i} - v_{k-1,i}) w_{1,i} + (v_{k-1,i} - v_{k-2,i}) w_{2,i} + \ldots + \\ &\quad + (v_{2,i} - v_{1,i}) w_{k-1,i}] \end{aligned} \tag{2.16}$$

The friction loss coefficient $\lambda$ in Eq. $(2.16)_1$ is expressed for the laminar flow by

$$\lambda = \frac{64}{\mathrm{Re}} \tag{2.17}$$

And for the turbulent flow, from Prandtl's formula, by

$$\frac{1}{\sqrt{\lambda}} = 0.869 \ln(\mathrm{Re}\sqrt{\lambda}) - 0.8 \tag{2.18}$$

The system of Eqs. (2.13)-(2.18) together with Eqs. (2.6), (2.9) and the boundary and initial conditions is the basis for creating an algorithm of calculations and then a computer program.

Figure 3 presents the algorithm of calculations.

### 2.4. Verification of the model

In order to compare the accuracy of unsteady and quasi-steady models of friction in relation to experimental data, simulations of a simple waterhammer case (tank – long liquid line and cut-off valve) were conducted.

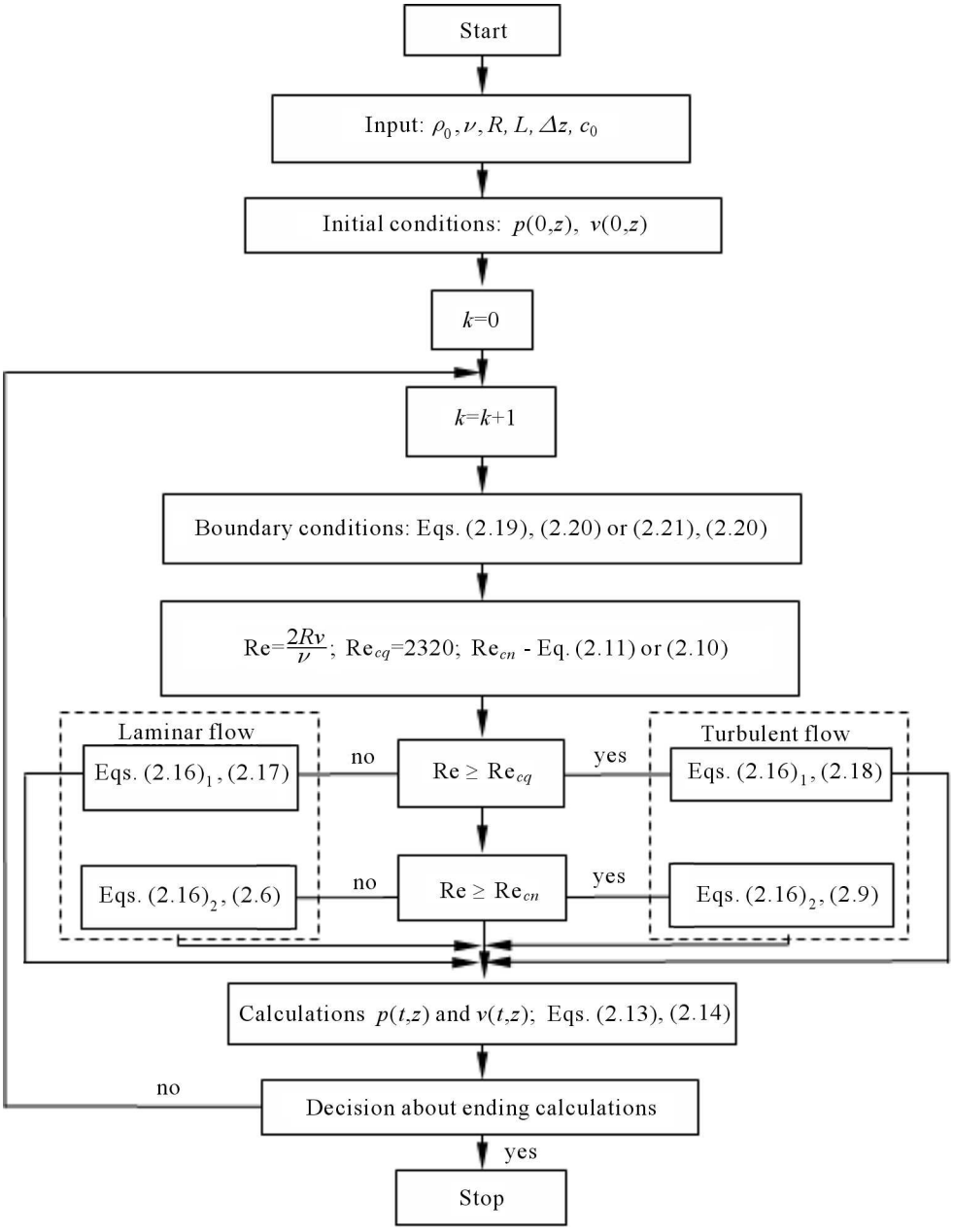


Fig. 3. Flow chart

The computed results were compared with experimental data reported by Holmboe and Rouleau (1967). They ran tests on a copper tube with radius 0.0127 m and length 36.1 m connected upstream to a tank which was maintained at a constant pressure by the compressed air. The liquid used in the experiment was an oil having viscosity $39.7 \cdot 10^{-6}\,\mathrm{m}^2/\mathrm{s}$. The measured sound speed was 1324 m/s and the initial flow velocity 0.128 m/s (Re = 82). The downstream valve was rapidly closed in the pipe line during flow. Pressure fluctuation was measured at the midpoint of the line. From the above parameters, it followed that it was a case of a laminar flow. It was determined in numerical calculations in which the models of Zielke, Eq. (2.4), and Schoohla (2.6) were used. In addition, the calculation with the quasi-steady model only i.e., with Eqs. $(2.16)_1$ and (2.17) was done as well.

Results of simulations and experimental data are shown in Fig. 4. It is clearly seen that the calculation using the weighting functions (changeable hydraulic resistance) is much closer to the experimental data. Therefore, in further calculations the weighting functions were used instead of the quasi-steady model.

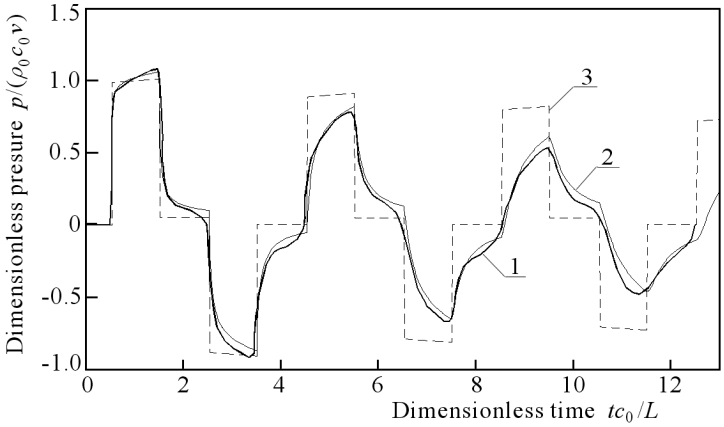


Fig. 4. Fluctuations of pressure at the midpoint of the line; 1 – experimental data, 2 – simulations with the unsteady model of friction, 3 – simulations with the quasi-steady model

### 2.5. Boundary conditions

It is necessary to know boundary conditions in order to be able to solve the system of Eqs. (2.1) and (2.4) using the method of characteristics. The analysis involves pressure runs at the beginning and at the end of the long line (Fig. 1) during a sudden shift of the hydraulic directional control valve in time $t_0$.

At that moment, a sudden change in the pressure from $p_0$ to $p_0 + \Delta p$ takes place. Two cases are investigated. The first case assumes a constant rate of delivery of the positive-displacement pump, the second one takes into account pulsation of the delivery of the pump. These conditions can be expressed in the following way:
— for a constant rate of delivery for $z = 0$

$$Q(t) = \text{ const} \tag{2.19}$$

and for $z = L$

$$p = \begin{cases} p_0 & \text{for} \quad 0 \leqslant t < t_0 \\ p_0 + \Delta p & \text{for} \quad t \geqslant t_0 \end{cases} \tag{2.20}$$

— for a changeable rate of delivery for $z = 0$

$$Q = Q_m \Big[1 - \frac{1}{2} \sum_{K=1}^{K=\infty} \delta Q_K \cos(\omega_K t)\Big] \tag{2.21}$$

where: $\omega_K$ denotes pulsations of harmonic vibration of the pump, $K$ – order of harmonics, $\delta Q_K$ – relative amplitudes of harmonic vibration of the flow rate according to the literature data, $Q_m$ – mean theoretical efficiency.

Relation (2.21) was obtained by Rohatynski (1968). The condition for $z = L$ has the form expressed in Eq. (2.20).

## 3. The test stand and description of experimental investigations

In order to validate the presented model and the method for simulation of the hydraulic waterhammer effect, some tests were carried out on a specially prepared test stand. A diagram of the hydraulic system of the test stand is presented in Fig. 5. The central part of the system comprised a hydraulic line. Two extensometer pressure converters (7), (9) of the working liquid were fixed to its two ends. The generated flow intensity through the axial-flow multipiston pump with deflected disc (6) Z-PTOZ2-K1-100R1 was measured by flowmeter (13). At the end of the hydraulic line, hydraulic control valve (10) (4/2) was installed, whose function was to suddenly direct the liquid through throttle valve (11). In order to realises an increase in the system load an adjustable throttle valve was used. To protect the system against an incidental and dangerous pressure increase, safety valve (8) was installed right at the pump.

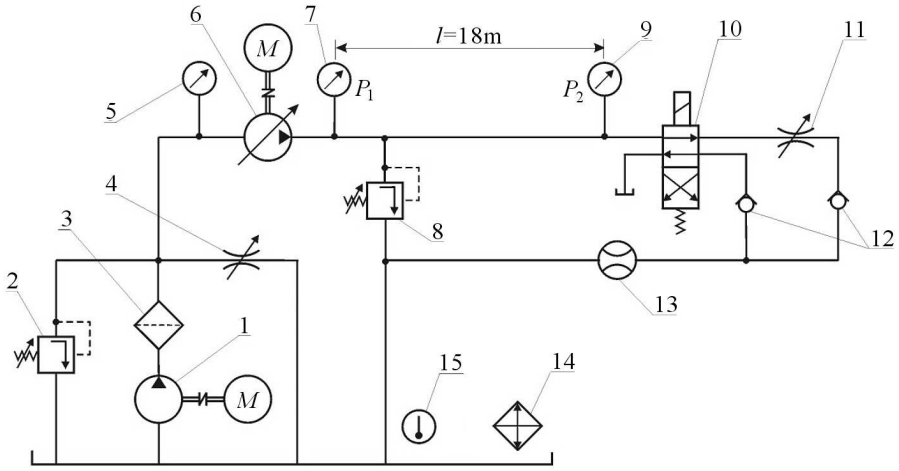


Fig. 5. A scheme of the hydraulic system used in experimental investigations on the pressure wave velocity propagation: 1 – hydraulic constant delivery pump (pressure charging pump), 2 – safety valve, 3 – filter, 4 – throttle valve, 5 – vacuometer, 6 – hydraulic variable displacement pump, 7 – pressure transducer, 8 – safety valve, 9 – pressure transducer, 10 – directional control valve 4/2, 11 – throttle valve, 12 – check valve, 13 – flowmeter, 14 – water cooler, 15 – thermometer

The unsteady state in the system was caused by the shifted hydraulic directional control valve directing the liquid flow through the throttle valve with higher hydraulic resistance $d_2$ (Fig. 1).

The time of shift of the directional control valve was $t_z = 20\,\text{ms}$. It was shorter than half of the hydraulic hammer time ($t_z < T/2 = 2L/c_0 = 0.028\,\text{s}$, $L = 18\,\text{m}$, $c_0 = 1309\,\text{m/s}$ which is determined in a further part of this paper).

The recording of the instantaneous pressure series at some points of the hydraulic line was carried out by means of measuring equipment consisting of tensometric pressure sensors, screened conductors eliminating the outside interference, digital oscilloscope Tektronix TDS-224, multi-channel signal amplifier TDA-6, computer with an analogue-digital card AD/DA and Wave Star-Tektronix software.

## 4. Spectroscopic analysis of pressure pulsation in the steady state

The recording of the pressure series in a steady state (before the shift of the directional control valve) was carried out in two measuring points: behind the

pump and in front of the control valve. The recorded time series are presented in Fig. 6. They display pressure pulsation resulting from the operation of the positive-displacement pump. The dominant pulsation frequency for the investigated system can be estimated from the following relation

$$f_K = \frac{n_p z K}{60} \text{ [Hz]} \tag{4.1}$$

where $n_p$ is the speed of rotation of the pump shaft [rev/min], $z$ – number of displacement elements, $K$ – number of harmonics, $K = 1, \ldots, n$.

The investigated system comprised an axial-flow multi-piston pump with a deflected disk of the type PTOZ-100 driven at the speed $n = 1500\,\text{rev/min}$ and containing $z = 9$ pistons, which according to relation (4.1) yields $f_1 = 225\,\text{Hz}$.

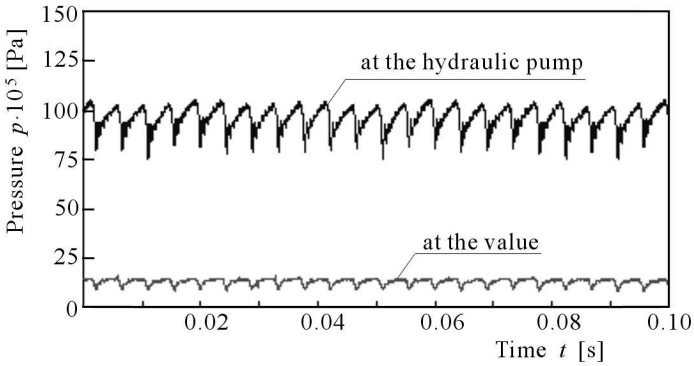


Fig. 6. The recorded time series during steady operation of the system. Data: $\nu = 100\,\text{cSt}$, mean pressure at the valve $p_0 = 1.2\,\text{MPa}$, mean intensity of the flow $Q = 50\,\text{dm}^3/\text{min}$

Additionally, on the basis of the time series, an FFT spectroscopic analysis of the pressure pulsation was carried out. Figure 7 presents the obtained results.

As it can be seen in the presented diagrams of pressure pulsation spectra, the dominant frequency in the analyzed series is the operational frequency of the positive-displacement pump. The first frequency $f_1$ is $225\,\text{Hz}$. The successive harmonics are respectively $f_2 = 450\,\text{Hz}$, $f_3 = 675\,\text{Hz}$, $f_4 = 900\,\text{Hz}$, ...

The analysis carried out during the investigations makes it possible to take into account the first harmonic in boundary condition (2.21), the harmonic resulting from kinematics of the pump. Higher frequencies require a much finer numerical grid, which very significantly decrease the efficiency of simulation (in our tests time of calculations was prolonged hundred times).

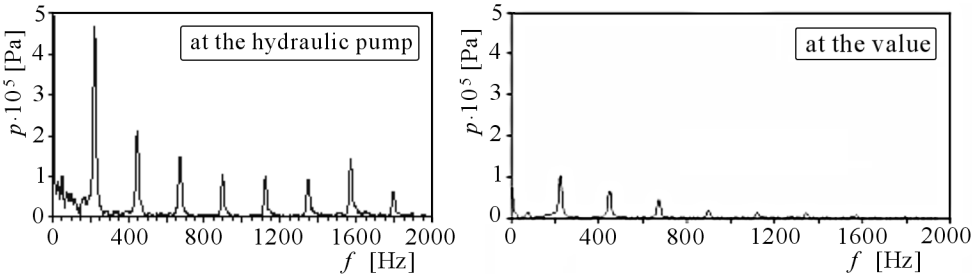


Fig. 7. Amplitude-frequency spectra of the pressure pulsation in the hydraulic system caused by the non-uniform delivery of the pump

## 5. Numerical and experimental results

As it was mentioned earlier, the series of pressure changes were investigated after a sudden shift of the control valve at measuring point 1 (at the control valve) and point 2 (at the pump).

The parameters of the line were as follows: length of the line $L = 18\,\mathrm{m}$, inner diameter of the line $d = 2R = 9\,\mathrm{mm}$, thickness of the line wall $g = 1.5\,\mathrm{mm}$, material of the line steel $E = 2.1 \cdot 10^{11}\,\mathrm{Pa}$.

The working liquid of the system was a hydraulic oil (HL 68) with density $\rho_0 = 860\,\mathrm{kg/m^3}$ and the modulus of volume elasticity $\beta_c = 1.5 \cdot 10^9\,\mathrm{Pa}$.

The speed of sound $c_0$ calculated according to Eq. (2.2) was $1309\,\mathrm{m/s}$.

The investigations were carried out for two variants:

- laminar flow: $\mathrm{Re} = 471$ $(\nu = 150\,\mathrm{cSt})$
- turbulent flow: $\mathrm{Re} = 2829$ $(\nu = 50\,\mathrm{cSt})$

In both variants, the delivery rate of the pump in the boundary condition could either be constant (Eq. (2.19)) or changeable (Eq. (2.21)).

The simulation investigations were carried out according to the algorithm presented in Fig. 3. The adopted number of the measured segments was $h = 20$, the length of the calculated segment $\Delta z = L/h = 0.9\,\mathrm{m}$ and the value of the time step $\Delta t = \Delta z/c_0 = 0.007\,\mathrm{s}$.

Figures 8-11, shown below, present both the recorded series and the expected series simulated numerically. In Figs. 7-10, numbers 1-4 correspond to:

1 – numerical simulation, pressure at the hydraulic pump

2 – pressure at the valve (the boundary condition in calculations)

3 – experimental data, pressure at the hydraulic pump

4 – experimental data, pressure at the valve.

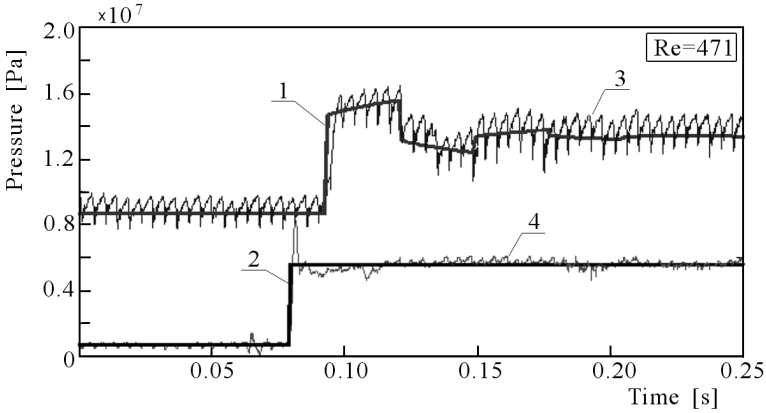


Fig. 8. Comparison between experimental and numerical results; $\nu = 150\,\mathrm{cSt}$, $Q = 30\,\mathrm{dm}^3/\mathrm{min}$, $p_0 = 0.7\,\mathrm{MPa}$, $L = 18\,\mathrm{m}$, $\Delta p = 4.9\,\mathrm{MPa}$ ($Q$ – mean intensity of the flow rate, $p_0$ – mean pressure at the valve before unsteady state)

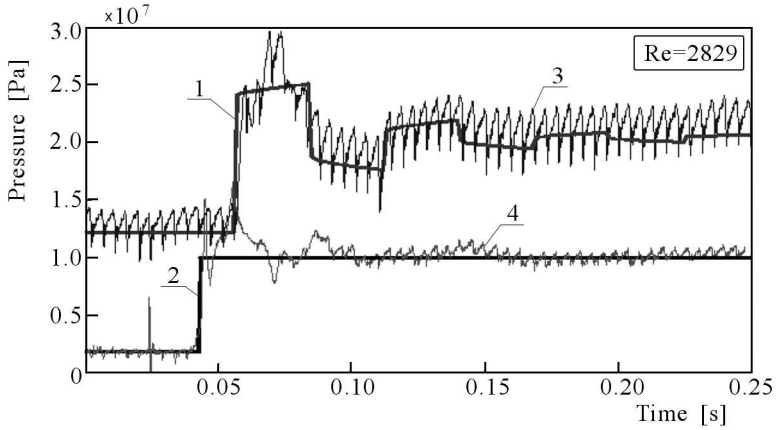


Fig. 9. Comparison between experimental and numerical results; $\nu = 50\,\mathrm{cSt}$, $Q = 60\,\mathrm{dm}^3/\mathrm{min}$, $p_0 = 1.85\,\mathrm{MPa}$, $L = 18\,\mathrm{m}$, $\Delta p = 7.8\,\mathrm{MPa}$

Using the above mentioned boundary conditions, numerical simulation was carried out. The obtained results were compared with those determined experimentally and presented in Fig. 10 and Fig. 11.

The verification assessment of the numerical results with the experimental data is problematic due to interference recorded during the experiment. As it can be seen in the comparisons presented in Figs. 8-11, the pressure pulsation resulting from the irregular operation of the pump greatly influences the recorded experimental series.

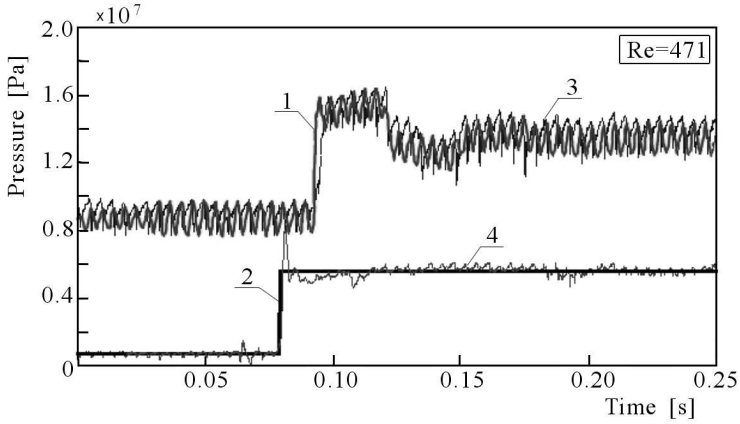


Fig. 10. Comparison between experimental and numerical results for the transient state with pulsating intensity of the liquid flow taken into account at the boundary condition; $\nu = 150\,\mathrm{cSt}$, $Q = 30\,\mathrm{dm}^3/\mathrm{min}$, $p_0 = 0.7\,\mathrm{MPa}$, $L = 18\,\mathrm{m}$, $\Delta p = 4.9\,\mathrm{MPa}$

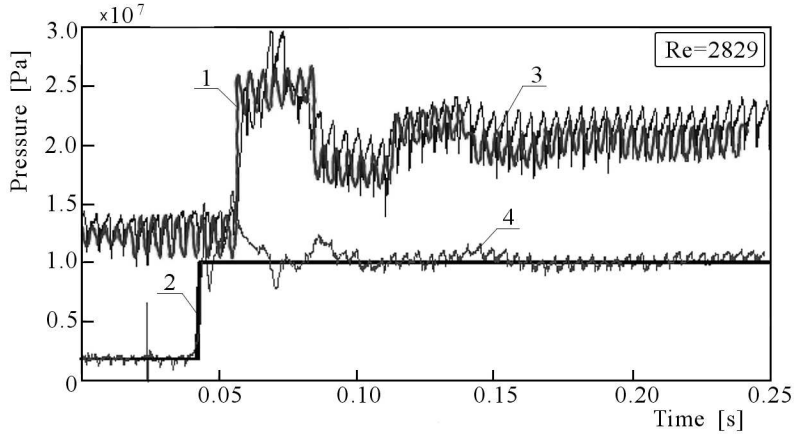


Fig. 11. Comparison between experimental and numerical results for the transient state with pulsating intensity of the liquid flow taken into account at the boundary condition; $\nu = 50\,\mathrm{cSt}$, $Q = 60\,\mathrm{dm}^3/\mathrm{min}$, $p_0 = 1.85\,\mathrm{MPa}$, $L = 18\,\mathrm{m}$, $\Delta p = 7.8\,\mathrm{MPa}$

We should not forget about other factors which may also influence the experiment. These include:

- changes in the viscosity and density of the liquid along the line caused by temperature changes of the flowing liquid. It should be remembered that while flowing through the hydraulic line, the temperature of the liquid, owing to friction, goes up by even a dozen or so degrees. The temperature increase is connected with some changes in properties of

the liquid. In order to minimize the influence the temperature may have on the results of the experiment, a water cooler was used

- the undissolved air found in the oil used in the hydraulic system may cause an interference and a time-lag of the phase series (Wylie and Streeter, 1978). In order to eliminate this interference, the exhaust line of the pump was equipped with the so-called supercharging pump, which ensured that in the exhaust area the pressure did not go below the pressure of air precipitation from the oil, which made it possible to avoid cavitation (Kollek *et al.*, 2003).
- fluid structure interactions may also lead to interferences in pressure changes
- the shift of the control valve directing the flow of the liquid through the throttle valve with a higher hydraulic resistance does not fully reflect the abrupt (rectangular) pressure changes at the control valve. Additional pressure oscillations appear as well (particularly at a high flow intensity and low viscosity). Most probably, they are due to very short but complete stoppage of the liquid flow during the shift of the control valve.

## 6. Concluding remarks

The following conclusions can be drawn from the tests that were carried out in this study:

- the application of the developed method for simulating transients while also taking into account unsteady friction resistance of the liquid (Eqs. (2.13)-(2.18) together with Eqs. (2.6) and (2.9)) provides a convenient method for effective numerical calculations for both laminar and turbulent flows
- in the registered pressure changes in the quasi-steady state, the pulsation of the delivery rate of the pump plays a significant role. It may cause pressure pulsation up to $\pm$10-20% of the mean pressure
- in the investigations of transient states caused by load changes of the hydraulic system resulting from a sudden change in the flow and directing it through the throttle valve with a higher hydraulic resistance, the pressure pulsation which results from the delivery pulsation significantly interferes and distorts the pressure changes

- if the pulsation of the hydraulic pump delivery is taken into account in the boundary conditions, it significantly brings the results of numerical simulations closer to the experimental data.

## Notation

| | | |
|---|---|---|
| $c_0$ | – | acoustic wave speed, [m/s] |
| $E$ | – | Young's modulus, [N/m$^2$] |
| $g$ | – | thickness of wall pipe, [m] |
| $f$ | – | frequency of the pulsation, [s$^{-1}$] |
| $L$ | – | pipe length, [m] |
| $m$ | – | number of time steps, [–] |
| $n_p$ | – | speed of rotation, [rpm] |
| $p$ | – | pressure, [Pa] |
| $R$ | – | radius of pipe, [m] |
| $\mathrm{Re}, \mathrm{Re}_{cn}$ | – | Reynolds number and critical Reynolds number, respectively, [–] |
| $T$ | – | period of waterhammer, [s] |
| $t$ | – | time, [s] |
| $\widehat{t} = \nu t/R^2$ | – | dimensionless time, [–] |
| $v$ | – | instantaneous mean flow velocity in the cross section, [m/s] |
| $w$ | – | weighting function, [–] |
| $z$ | – | distance along pipe axis, [m] |
| $\beta_c$ | – | bulk modulus of the liquid, [Pa] |
| $\lambda$ | – | Darcy-Weisbach friction coefficient, [–] |
| $\mu$ | – | dynamic viscosity, [kg m$^{-1}$s$^{-1}$] |
| $\nu$ | – | kinematic viscosity, [m$^2$s$^{-1}$] |
| $\rho_0$ | – | fluid density (constant), [kg m$^{-3}$] |
| $\tau_w, \tau_{wq}, \tau_{wu}$ | – | wall shear stress, wall shear stress for quasi-steady flow and unsteady wall shear stress, respectively, [kg m$^{-1}$s$^{-2}$] |
| $\omega$ | – | angular frequency of the pulsation, [s$^{-1}$] |
| $\Omega = \omega R^2/\nu$ | – | dimensionless frequency, [–] |

## References

1. CHAUDHRY M.H., HUSSAINI M.Y., 1985, Second-order explicit finite-difference schemes for waterhammer analysis, *Journal of Fluids Engineering*, **107**, 523-529

2. GARBACIK A., SZEWCZYK K., 1995, *New Aspects of Modelling of Fluid Power Control*, Wrocław, Warszawa, Kraków, Ossolineum

3. HOLMBOE E.L., ROULEAU W.T., 1967, The effect of viscous shear on transiets in liquid lines, *Transactions ASME, Journnal of Basic Engineering*, **89**, 11, 174-180

4. JELALI M., KROLL A., 2003, *Hydraulic Servo-systems. Modelling, Identification and Control*, Springer-Verlag, London

5. JUNGOWSKI W., 1976, *One-dimensional Transient Flow*, Publishing House of Warsaw University of Technology [in Polish]

6. KOLLEK W., KUDŹMA Z., STOSIAK M., 2003, Acoustic diagnostic testing in identification of phenomena associated with flow of working medium in hydraulic systems [in Polish], *Twelve Power Seminar '2003 on Current Flow, Design and Operational Problems of Hydraulic Machines and Equipment*, Gliwice, Poland

7. KUDŹMA S., 2005, Modeling and simulation dynamical runs in closed conduits of hydraulics systems using unsteady friction model, PhD work at Szczecin University of Technology, February [in Polish]

8. OHMI M., KYONEN S., USUI T., 1985, Numerical analysis of transient turbulent flow in a liquid line, *Bulletin of JSME*, **28**, 239, 799-806

9. RAMAPRIAN B.R., TU S.-W., 1980, An experimental study of oscillatory pipe flow at transitional Reynolds number, *J. Fluid Mech.*, **100**, 3, 513-544

10. ROHATYŃSKI R., 1968, *Damping of Pressure Pulsations in Hydraulic Systems with Displacement Pumps*, Scientific Work of Wroclaw University of Technology, No. 191, Power Engineering IX [in Polish]

11. SCHOHL G.A., 1993, Improved approximate method for simulating frequency-dependent friction in transient laminar flow, *Journal of Fluids Eng., Trans. ASME*, **115**, 420-424

12. TRIKHA A. K., 1975, An efficient method for simulating frequency-dependent friction in transient liquid flow, *Journal of Fluids Eng., Trans. ASME*, 97-105

13. VARDY A.E., BROWN J., 1996, On turbulent, unsteady, smooth-pipe friction, *Proc. of 7th International Conference on Pressure Surges*, Harrogate UK, 16-18, BHRA Fluid Eng., 289-311

14. VARDY A.E., BROWN J.M.B., KUO-LUN H., 1993, A weighting function model of transient turbulent pipe flow, *J. Hyd. Res.*, **31**, 4, 533-548

15. WYLIE E.B., STREETER V.L., 1978, *Fluid Transients*, McGraw-Hill, New York

16. ZARZYCKI Z., 1994, *A Hydraulic Resistances of Unsteady Lquid Flow in Pipes*, Scientific Works at Szczecin University of Technology, No. 516, Szczecin

17. ZARZYCKI Z., 2000, On weighting function for wall shear stress during unsteady turbulent pipe flow, *8th International Conference on Pressure Surges*, BHR Group, The Hague, 529-543

18. ZARZYCKI Z., KUDŹMA S., 2004, Simulations of transient turbulent flow in liquid lines using time-dependent frictional losses, *The 9th International Conference on Pressure Surges*, BHR Group, Chester, UK, 24/26, 439-455

19. ZARZYCKI Z., KUDŹMA S., 2005, Computation of transient turbulent flow of liquid in pipe using unsteady friction formula, *Transactions of the Institute of Fluid – Flow Machinery*, **116**, 27-42

20. ZIELKE W., 1968, Frequency-dependent friction in transient pipe flow, *Journal of Basic Eng., Trans. ASME*, 109-115

## Symulacja przepływów przejściowych w układzie hydraulicznym z hydrauliczną linią długą

Streszczenie

Artykuł przedstawia zagadnienie modelowania i symulacji zjawisk przejściowych w układach hydraulicznych z hydrauliczną linią długą. Wykorzystano model tarcia niestacjonarnego do opisu niestacjonarnego przepływu w przewodzie. Naprężenia ścinające na ściankach przewodów są określone za pomocą przyspieszenia i finkcji wagi, która zależy od charakteru przepływu (uwarstwiony, turbulentny). Rezultaty symulacji numerycznych są prezentowane dla uderzenia hydraulicznego, które spowodowane jest poprzez nagłe przesterowanie rozdzielacza. Rozpatrywane są dwa przypadki: pierwszy – gdy układ zasilający podaje stałą wartość natężenia przepływu, drugi – uwzględniający pulsację wydajności pompy wyporowej. Symulacje komputerowe są porównane z wynikami badań eksperymentalnych. Wykazano dużą zgodność symulacji komputerowych uwzględniających pulsację wydajności pompy z wynikami eksperymentu.

*Manuscript received March 9, 2007; accepted for print April 25, 2007*